Available online at www.sciencedirect.com
ScienceDirect
Carbohydrate Polymers 69 (2007) 713–724
Carbohydrate Polymers
www.elsevier.com/locate/carbpol

"Melt-in-the-mouth" gels from mixtures of xanthan and konjac glucomannan under acidic conditions: A rheological and calorimetric study of the mechanism of synergistic gelation

A.A. Agoub [a], A.M. Smith [b,1], P. Giannouli [c], R.K. Richardson [b], E.R. Morris [a,*]

[a] *Department of Food and Nutritional Sciences, University College Cork, Cork, Ireland*
[b] *Cranfield University at Silsoe, Silsoe, Bedford MK45 4DT, UK*
[c] *Department of Biochemistry and Biotechnology, University of Thessaly, Larissa, Greece*

Received 12 December 2005; received in revised form 18 December 2006; accepted 12 February 2007
Available online 21 February 2007

Abstract

The effect of acidification on a typical commercial xanthan and on pyruvate-free xanthan (PFX), alone and in gelling mixtures with konjac glucomannan (KGM), has been studied by differential scanning calorimetry (DSC) and small-deformation oscillatory measurements of storage modulus (G') and loss modulus (G''). For both xanthan samples, progressive reduction in pH caused a progressive increase in temperature of the disorder–order transition in DSC, and a progressive reduction in gelation temperature with KGM. This inverse correlation is interpreted as showing that synergistic gelation involves disruption of the xanthan 5-fold helix, probably by attachment of KGM to the cellulosic backbone of the xanthan molecule (as proposed previously by a research group in the Institute of Food Research, Norwich, UK). Higher transition temperature accompanied by lower gelation temperature for PFX in comparison with commercial xanthan at neutral pH is explained in the same way. However, an additional postulate from the Norwich group, that attachment of KGM (or galactomannans) can occur only when the xanthan molecule is disordered, is inconsistent with the observation that gelation of acidified mixtures of KGM with PFX can occur at temperatures more than 60 °C below completion of conformational ordering of the PFX component (as characterised by DSC). Increase in G' on cooling for mixtures of commercial xanthan with KGM at pH values of 4.5 and 4.25 occurred in two discrete steps, the first following the temperature-course observed for the same mixtures at neutral pH and the second occurring over the lower temperatures observed for mixtures of KGM with PFX at the same values of pH. These two "waves" of gel formation are attributed to interaction of KGM with, respectively, xanthan sequences that had retained a high content of pyruvate substituents, and sequences depleted in pyruvate by acid hydrolysis. At pH values of ~4.0 and lower, gelation of mixtures of KGM with commercial xanthan followed essentially the same temperature-course as for mixtures with PFX, indicating extensive loss of pyruvate under these more strongly acidic conditions. Mixtures prepared at pH values in the range 4.0–3.5 gave comparable moduli at room temperature (20 °C) to those obtained at neutral pH, but showed substantial softening on heating to body temperature, suggesting possible applications in replacement of gelatin in products where "melt-in-the-mouth" characteristics are important for acceptability to the consumer.

Keywords: Xanthan; Konjac; Gelation; Gelatin replacement; Rheology; DSC

1. Introduction

Xanthan, the extracellular bacterial polysaccharide from *Xanthomonas campestris*, has a linear cellulosic backbone solubilised by charged trisaccharide sidechains attached at O(3) of alternate glucose residues, to give a pentasaccharide

* Corresponding author. Tel.: +353 21 4903625; fax: +353 21 4270001.
E-mail address: ed.morris@ucc.ie (E.R. Morris).
[1] Present address: Biomaterials Unit, University of Birmingham, School of Dentistry, St. Chad's Queensway, Birmingham B4 6NN, UK.

0144-8617/$ - see front matter © 2007 Elsevier Ltd. All rights reserved.
doi:10.1016/j.carbpol.2007.02.014

repeating sequence. The sidechains have the structure: β-D-Man*p*-(1 → 4)-D-GlcA*p*-(1 → 2)-D-Man*p*-1 → with variable, non-stoichiometric substitution by *O*-acetate at C(6) of the inner mannose and 4,6-linked pyruvate ketal groups on terminal mannose residues (Jansson, Kenne, & Lindberg, 1975; Melton, Mindt, Rees, & Sanderson, 1976).

At high temperature and low ionic strength xanthan exists in solution as a disordered coil, but on cooling and/or addition of salt it undergoes a co-operative conformational transition to a rigid, ordered structure (Holzwarth, 1976; Milas & Rinaudo, 1979, 1986; Morris, 1973; Morris, Rees, Young, Walkinshaw, & Darke, 1977; Norton, Goodall, Frangou, Morris, & Rees, 1984). It is well established that the ordered structure is a 5-fold helix (Moorhouse, Walkinshaw, & Arnott, 1977; Okuyama et al., 1980), but there is some controversy over whether the helix is a single-stranded structure stabilised by ordered packing of sidechains along the polymer backbone, or a co-axial double helix. The disorder–order transition is fully reversible, with no detectable thermal hysteresis. As anticipated from polyelectrolyte theory (Piculell & Nilsson, 1990), adoption of the ordered structure is promoted by increasing ionic strength, with consequent increase in the midpoint temperature (T_m) of the conformational transition.

Solutions of ordered xanthan flow freely, but at concentrations above ~0.3% w/v they have obvious gel-like character. In small-deformation oscillatory measurements, elastic response (storage modulus, G') substantially exceeds viscous flow (loss modulus, G'') and both moduli show only limited variation with frequency, as in conventional gels. These ''weak gel'' properties (Ross-Murphy, 1984; Ross-Murphy, Morris, & Morris, 1983) are attributed to tenuous association of ordered chains.

Xanthan can, however, form self supporting gels when mixed with galactomannans of low galactose content, notably locust bean gum (LBG), or with konjac glucomannan (KGM). Like xanthan, these polysaccharides have a primary structures based on a linear backbone of (1 → 4)-diequatorially-linked pyranose sugars. KGM is obtained from the tubers of *Amorphophallus konjac* and related species. The polymer backbone contains both β-D-mannose and β-D-glucose residues, in the approximate ratio 2:1, with no long blocks of either type (Davé & McCarthy, 1997; Nishinari, Williams, & Phillips, 1992). Solubility is conferred by *O*-acetyl substituents on a proportion (5–10%) of the constituent sugars, and by some limited branching. Galactomannans occur in the seed endosperm of a wide range of leguminous plants. The polymer backbone consists exclusively of β-D-mannose, with α-D-galactose attached as irregularly-spaced single-sugar sidechains at O(6) of a proportion of the mannose residues (Dea & Morrison, 1975).

The ratio of mannose to galactose varies widely between different galactomannans. Like cellulose, unsubstituted mannan is totally insoluble in water (although it can be dissolved in strong alkali) and the solubility of the galactomannans decreases with decreasing galactose content. The ability of galactomannans to form synergistic gels with xanthan also increases with decreasing galactose content, prompting an early suggestion (Morris et al., 1977) that the gel network is formed by attachment of unsubstituted regions of the mannan backbone to the surface of the xanthan 5-fold helix. A similar model was proposed for attachment of KGM to the xanthan helix (Dea et al., 1977). Subsequently, however, it has been suggested that intermolecular association involves attachment of the plant polysaccharide to the cellulosic backbone of the xanthan molecule, rather than to the 5-fold helix, and occurs only when the xanthan chain is in the disordered state (Brownsey, Cairns, Miles, & Morris, 1988; Cairns, Miles, & Morris, 1986; Cairns, Miles, Morris, & Brownsey, 1987; Morris, 1992). Although differing substantially, both of these models invoke direct binding between the constituent polysaccharides.

However, interactions between different polymers can also arise from thermodynamic incompatibility (Morris, 1990; Tolstoguzov, 1991), either by phase-separation (which raises the effective concentration of both components) or by exclusion effects that promote self-association within a single phase, but there is strong evidence that gelation of xanthan with galactomannans or KGM does not occur in this way. First, maximum interaction occurs (Goycoolea, Richardson, Morris, & Gidley, 1995) at a specific stoichiometric ratio of the two polymers, independent of their total concentration, as would be expected for a binding process, whereas the effects of thermodynamic incompatibility normally become increasingly apparent as the concentration of either or both components is raised. Also, strong interaction can be detected at very low polymer concentrations, where polymer incompatibility would be expected to have negligible effect (Goycoolea, Foster, Richardson, Morris, & Gidley, 1994). Perhaps the most direct evidence of binding, however, is that (partially depolymerised) LBG has been observed to co-elute with xanthan in gel permeation chromatography of mixed solutions (Cheetham, McCleary, Teng, Lum, & Maryanto, 1986).

Virtually all previous studies of the synergistic gelation of xanthan with galactomannans or KGM have been carried out at neutral pH. It has, however, been observed that formation of xanthan–LBG gels is inhibited or abolished under acidic conditions. This behaviour is described in a patent (Pramoda & Lin, 1979), but does not appear to have been explored further. The aim of the present investigation was to determine whether or not similar inhibition occurs for mixtures of xanthan with KGM, and to explore the underlying mechanism. Preliminary accounts of some aspects of the work have been presented elsewhere (Fitzsimons, Agoub, Giannouli, Mulvihill, & Morris, 2005; Smith, 2002).

2. Materials and methods

Two xanthan samples were used: a typical food-grade commercial material (Keltrol T from CP Kelco, San Diego,

CA, USA) and pyruvate-free xanthan (PFX), prepared from genetically-engineered *X. campestris*, which was kindly supplied as a research sample by CP Kelco. Konjac glucomannan (KGM) from Senn Chemicals AG was identical to the material used by Goycoolea et al. (1995). Stock solutions of each polymer, at the same concentration, were prepared in distilled deionised water and were acidified to pH 2.0 by addition of 1 M HCl. Aliquots were then adjusted to the required pH (within the range 2.5–7.0) by addition of 1 M KOH, to maintain the same ionic strength in all samples. Mixtures were prepared by combining equal volumes of the individual polymer solutions.

Rheological measurements were made using cone and plate geometry (5 cm diameter; 0.05 rad cone angle) on a sensitive prototype rheometer designed and constructed by one of us (R.K.R.). Samples were loaded at ~85 °C, and were coated around their periphery with light silicone oil, to minimise loss of water. Temperature was controlled by a circulating water bath and measured by a thermocouple in direct contact with the stationary element.

Differential scanning calorimetry (DSC) measurements were made using a sample mass of 865 ± 8 mg and fixed scan rate of 0.5 °C/min on a Seteram DSC III microcalorimeter, with water as thermal reference. Sample and reference pans were balanced to within 0.5 mg. Baselines were interpolated by fitting a polynomial function (normally second-order) to the experimental curves at temperatures above and below the range of the thermal transition. After subtraction of baselines, peak areas were calculated by numerical integration, and were converted to transition enthalpy by the following relationship:

$$\Delta H = 6000A/Rcm \quad (1)$$

where A is peak area (mW °C), R is scan rate (°C/min), c is polymer concentration (wt%), m is mass of solution used (mg) and ΔH is transition enthalpy (J/g). The values obtained are listed in Table 1, and are discussed in Section 4. For mixtures of KGM with PFX, ΔH is expressed in joules per gram of the xanthan component, to allow direct comparisons to be made with ΔH values obtained for the conformational transition of xanthan alone (commercial and pyruvate-free).

Table 1
Enthalpy changes from DSC

pH	ΔH (J/g xanthan)		
	Xanthan[a] alone	PFX alone	PFX + KGM
3.00			4.5
3.50	7.3		4.5
3.75	7.0		
4.00	9.2	6.5	4.2
4.50	9.1	6.5	
7.00	7.5	7.5	5.3
Mean	8.0	6.9	4.6
SD	1.0	0.6	0.5

[a] Keltrol T.

3. Results

As shown in Fig. 1, gelation of KGM in combination with commercial xanthan on cooling at neutral pH is characterised by a sharp increase in G' and G'' at ~60 °C, with both moduli levelling out towards constant values at temperatures below ~35 °C. Closely similar results have been reported previously (e.g. Goycoolea et al., 1995), and it has been shown that the gelation process is fully reversible on heating, with no thermal hysteresis beyond that expected from thermal lag (i.e. from the temperature in the interior of the sample trailing slightly behind the measured temperature at the plates of the rheometer during cooling and heating).

The effect of reduction in pH on the changes in G' during cooling is shown in Fig. 2a; the accompanying changes in G'' are shown in Fig. 2b. At pH 4.75, the temperature-dependence of both moduli is broadly similar to that observed (Fig. 1) at pH 7, although the final values on completion of cooling to 5 °C are slightly lower. However, on further reduction in pH to 4.5, increase in G' occurs in two steps, one beginning at ~60 °C, as at neutral pH (Fig. 1), and the other at ~45 °C. Essentially the same pattern is observed at pH 4.25, but with now a discernable step in G'' over the same temperature-range as the second increase in G'. At pH 4.0, the increase in G' and G'' at ~45 °C becomes the dominant process, with no indication of the sharp rise in moduli at ~60 °C which is seen at higher pH; there is, however, evidence of a transition at higher temperature, with G' rising above G'' at ~75 °C. As the pH is decreased further, to 3.5, 3.0 and 2.5, there is a progressive increase in the temperature at which G' first exceeds G'', and a progressive decrease in the temperature of the subsequent rise in both moduli, until eventually, at pH 2.5, this second (gelling) transition is abolished (or

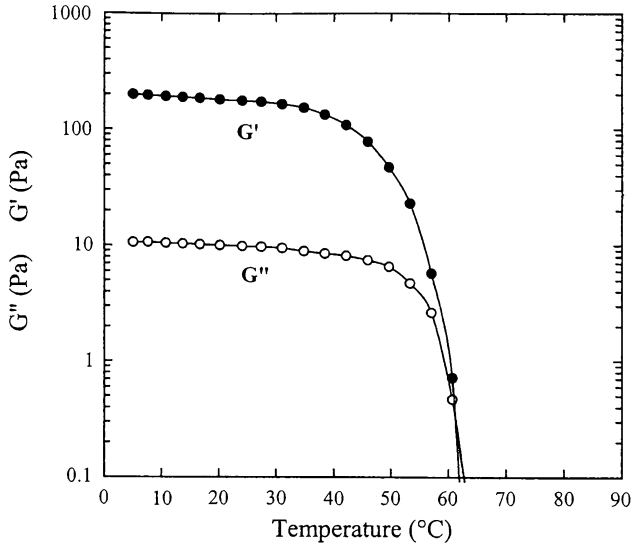

Fig. 1. Changes in G' (●) and G'' (○), measured at 1 rad s^{-1} and 1% strain, for 0.25 wt% commercial xanthan in combination with 0.25 wt% KGM on cooling (1.0 °C/min) at pH 7.0.

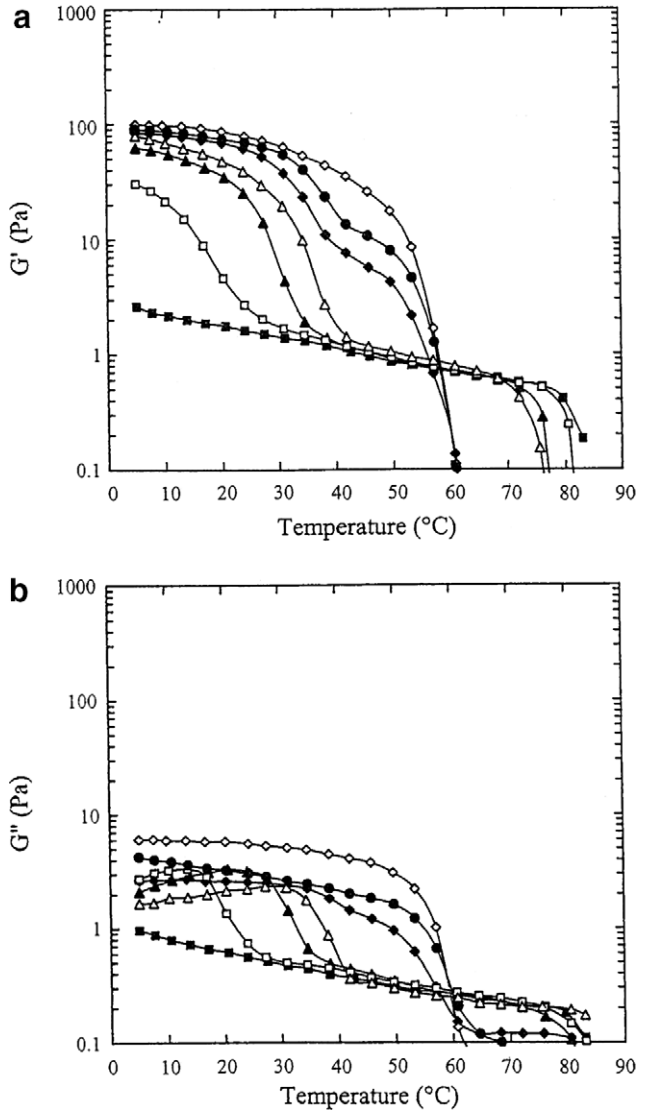

Fig. 2. Changes in (a) G' and (b) G'' observed for 0.25 wt% commercial xanthan in combination with 0.25 wt% KGM on cooling (1.0 °C/min) at pH values of 4.75 (◇), 4.5 (●), 4.25 (◆), 4.0 (△), 3.5 (▲), 3.0 (□) and 2.5 (■).

displaced to below 5 °C), which accords with the loss of synergistic gelation at low pH observed by Pramoda and Lin (1979) for mixtures of xanthan with LBG.

In summary, the results presented in Fig. 2 show (i) a sharp increase in G' in the early stages of cooling, which occurs at ~75 °C for the mixture prepared at pH 4.0 and moves to progressively higher temperature on further decrease in pH; (ii) a systematic reduction in gelation temperature as pH is lowered; and (iii) two "waves" of increase in G' at pH 4.5 and 4.25. When this complex behaviour was first observed (Smith, 2002) we could see no convincing, unified interpretation. It seemed possible, however, that one of the two waves of increase in G' might be due to displacement of the disorder–order transition of the xanthan component into the temperature-range of the sol–gel transition for mixtures with KGM. This possibility was explored by using DSC to monitor the effect of pH on the temperature-course of conformational ordering by xanthan alone. The DSC cooling curves obtained are shown in Fig. 3. It is evident that the transition, rather than being displaced to the lower temperatures where gelation occurs, moves to progressively higher temperature with decreasing pH until, at pH 3.25, it is obscured by the "start-up kick" of the calorimeter (thermal imbalance on initiation of cooling).

Conformational ordering, and associated development of xanthan "weak gel" structure ($G' > G''$), at progressively higher temperature as pH is decreased offers a simple explanation of the initial sharp increases in G' observed (Fig. 2) for the xanthan–KGM mixtures on cooling under acidic conditions (which also move to higher temperature with decreasing pH). It does not, however, help to explain the two "waves" of increase in G' seen for the mixtures prepared at pH 4.5 and 4.25, but another observation made in the DSC studies of commercial xanthan in the absence of KGM provided a starting point for understanding this phenomenon.

Previous studies (e.g. Goycoolea et al., 1995; Morris et al., 1977) have shown that, at neutral pH, the conformational transition of xanthan is completely reversible, with no thermal hysteresis beyond that expected from thermal lag, and is highly reproducible in repeated cycles of heating and cooling. Substantial departures from simple thermal reversibility were, however, observed under the acidic conditions studied in the present work. Fig. 4 shows DSC traces recorded for commercial xanthan on heating, cooling and re-heating (0.5 °C/min) at pH 3.5. There is a systematic increase in peak-maximum temperature, from

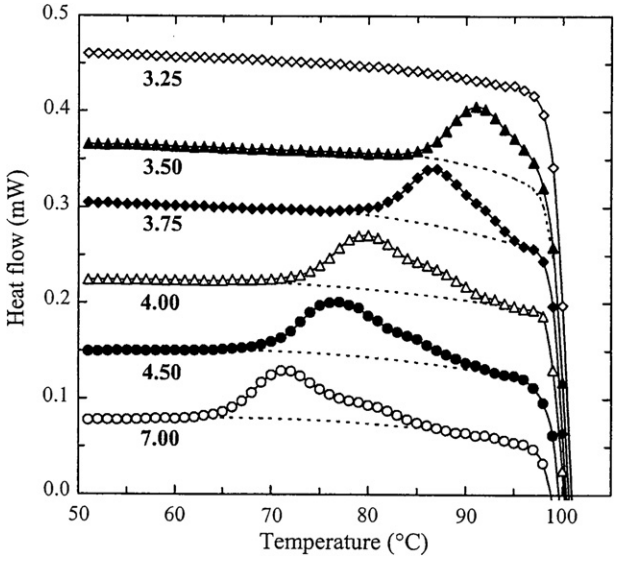

Fig. 3. DSC cooling scans (0.5 °C/min) for 1.0 wt% commercial xanthan at pH values of 7.0 (○), 4.5 (●), 4.0 (△), 3.75 (◆), 3.5 (▲) and 3.25 (◇). The dotted curves show interpolated baselines used in calculation of peak area. For clarity of presentation, the individual traces have been displaced vertically by arbitrary amounts.

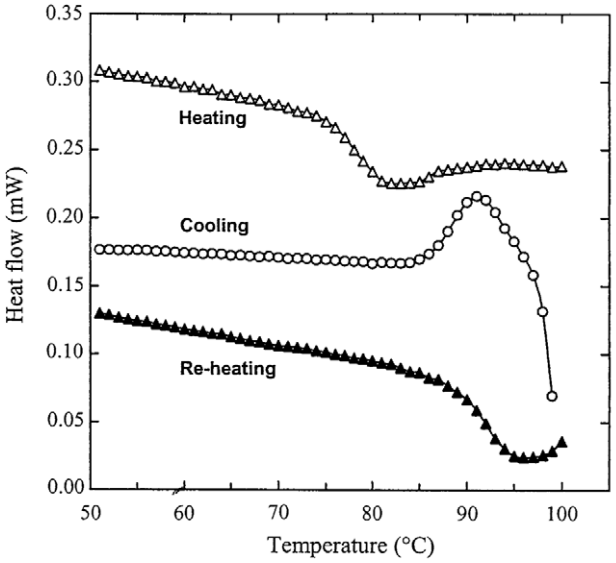

Fig. 4. DSC curves obtained for 1.0 wt% commercial xanthan at pH 3.5 on heating (△), cooling (○) and re-heating (▲) at 0.5 °C/min. For clarity of presentation, the individual traces have been displaced vertically by arbitrary amounts.

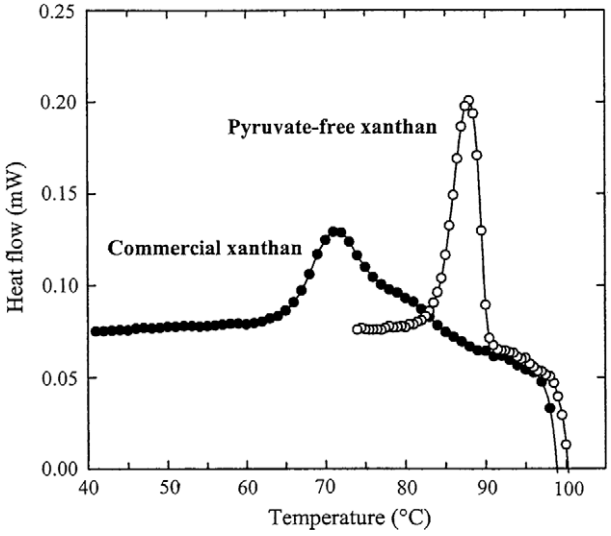

Fig. 5. DSC cooling scans (0.5 °C/min; pH 7.0) for 1.0 wt% solutions of PFX (○) and commercial xanthan (●).

~82 °C on initial heating, to ~91 °C on cooling, and ~96 °C in the second heating scan, suggesting a progressive change in primary structure during thermal cycling. The most obvious interpretation is loss of pyruvate ketal substituents by acid hydrolysis at high temperature and low pH.

The acetate substituents of xanthan, which are particularly susceptible to alkaline hydrolysis (Bradshaw, Nisbet, Kerr, & Sutherland, 1983), appear to contribute to the stability of the ordered structure, since their removal lowers the temperature of the order–disorder transition (Callet, Milas, & Rinaudo, 1987; Goycoolea et al., 1995). Pyruvate substituents, by contrast, are more susceptible to acid hydrolysis (Bradshaw et al., 1983) and reduce the stability of the ordered structure (Callet et al., 1987; Smith, Symes, Lawson, & Morris, 1981), presumably by introducing additional electrostatic repulsions between the trisaccharide sidechains of the xanthan molecule and by increasing the length of the sidechains and thus increasing the loss of entropy associated with conformational ordering. Removal of pyruvate groups therefore raises the temperature of the disorder–order transition, which could explain the progressive shift to higher temperatures shown in Fig. 4. This interpretation, and its possible implications for synergistic gelation, was pursued by investigation of the behaviour of pyruvate-free xanthan (PFX), alone and in gelling mixtures with KGM.

Fig. 5 shows a direct comparison of DSC cooling traces recorded for PFX and commercial xanthan at neutral pH. As anticipated, the transition temperature for the pyruvate-free sample is substantially higher than that of the commercial material (~88 °C in comparison with ~72 °C). Fig. 6a shows the effect of reduction in pH on DSC heating scans recorded for solutions of PFX; the cooling scans for the same solutions are shown in Figs. 6b and Fig. 7 shows the same DSC peaks after subtraction of interpolated baselines. As found for commercial xanthan (Fig. 3), the conformational transition of PFX moves to progressively higher temperature with decreasing pH (Fig. 6) until, at pH 3.5, it is displaced to above 100 °C.

The DSC peaks obtained on heating are closely similar in form and magnitude (Fig. 7) to those obtained on cooling, but occur at slightly higher temperature (by ~2 °C), which can be readily explained by thermal lag of ~1 °C in each direction of temperature change. The absolute values of heat flow for the heating and cooling peaks of each sample (Fig. 7) were averaged, and the temperature-course of conformational change (Fig. 8a) was obtained by numerical integration. The same procedure of numerical integration after subtraction of interpolated baselines was applied to the DSC traces obtained for commercial xanthan (Fig. 3); the resulting integrals are shown in Fig. 8b. Transition-midpoint temperature (T_m) for each solution was then obtained as the temperature at which 50% of the enthalpy change had occurred. The resulting values of T_m are shown in Fig. 9, plotted against pH. The increase in T_m on going from pH 7.0 to pH 4.5 is approximately the same (~5 °C) for commercial xanthan and PFX, but at lower pH the values of T_m for the commercial sample rise steeply towards the higher values observed for the pyruvate-free material, consistent with progressive loss of pyruvate groups by acid hydrolysis as the acidity of the solutions is increased.

It may be noted that for commercial xanthan at pH values of 4.0 and below the initial increase in G' on cooling in the presence of KGM (Fig. 2a), attributed to conformational ordering of the xanthan component in the mixtures, occurs at lower temperature than the onset of the disorder–order transition of xanthan alone over the same range of pH values, as monitored by DSC (Fig. 3). This can be

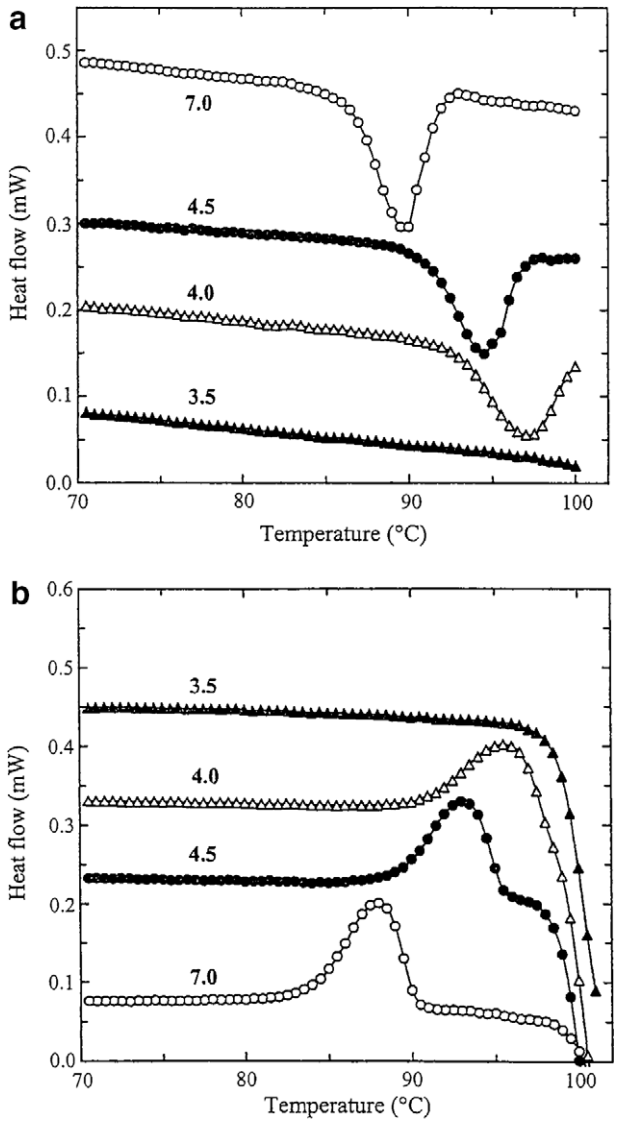

Fig. 6. DSC curves obtained for 1.0 wt% PFX on (a) heating and (b) cooling (0.5 °C/min) at pH values of 7.0 (○), 4.5 (●), 4.0 (△) and 3.5 (▲). For clarity of presentation, the individual traces have been displaced vertically by arbitrary amounts.

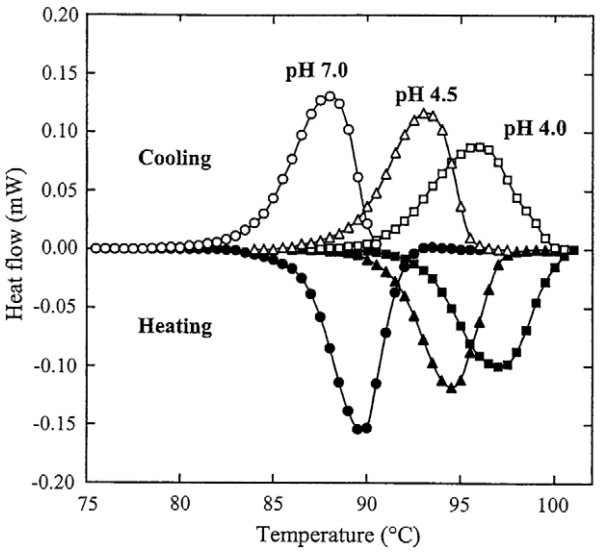

Fig. 7. DSC curves (0.5 °C/min; Fig. 6), after subtraction of interpolated baselines, for 1.0 wt% PFX on heating (filled symbols) and cooling (open symbols) at pH values of 7.0 (circles), 4.5 (triangles) and 4.0 (squares).

readily explained by differences in the time–temperature regimes used in the two sets of experiments. In the DSC studies, samples were loaded at ambient temperature, to avoid damage to the calorimeter, and heated to 100 °C at 0.5 °C/min before the cooling traces shown in Fig. 3 were recorded (also at a scan rate of 0.5 °C/min). The mixtures used in the rheological studies (Fig. 2), by contrast, were heated directly to 85 °C, loaded onto the rheometer, and cooled immediately at 1 °C/min, with therefore much shorter exposure of the xanthan component to acidic conditions at high temperature. It seems reasonable to conclude that this would lead to smaller reductions in pyruvate content and therefore to lower transition temperatures, as observed.

Fig. 10 shows the changes in G' and G'' observed for 0.5 wt% PFX on heating and cooling in the presence of an equal concentration of KGM (0.5 wt%) at neutral pH. On cooling, the steep increase in both moduli on formation of the mixed gel network begins at ~46 °C, substantially lower than the value of ~60 °C observed (Fig. 1) for KGM with commercial xanthan at the same pH (7.0). At temperatures above the onset of gelation, G' is already substantially higher than G''; this would be expected since, as shown in Fig. 8a, conformational ordering of PFX (with associated development of "weak gel" structure) is complete by ~80 °C at pH 7.0. The changes in moduli on heating (Fig. 10) are closely similar in form to those observed on cooling, but displaced to slightly higher temperature (by ~2 °C), which can again be explained by thermal lag. The same separation was observed at all pH values studied, and averaged values of moduli from cooling and heating scans are shown in Fig. 11 for G' (Fig. 11a) and G'' (Fig. 11b).

As observed (Fig. 2) for mixtures of KGM with commercial xanthan, gelation of KGM with PFX (Fig. 11) moves to progressively lower temperature with decreasing pH in the range 7.0–3.0. On further reduction in pH to 2.5 (Fig. 12) gel formation is abolished (or, perhaps, can be seen only as a slight up-turn in moduli below ~10 °C).

Fig. 13 shows DSC traces obtained for the same mixtures of KGM and PFX on heating (Fig. 13a) and cooling (Fig. 13b). In both directions of temperature change, the DSC peaks move to progressively lower temperature with decreasing pH, paralleling the reduction in gelation temperature observed rheologically (Fig. 11), until, at pH 2.5, no transitions are seen, indicating that they have been displaced to below the temperature-range of the DSC scans (i.e. to below 10 °C). As found in the DSC studies of PFX alone (Fig. 7), the peaks obtained on heating (Fig. 13a) are closely similar in form and magnitude to those obtained on cooling (Fig. 13b), but occur at slightly higher temperature

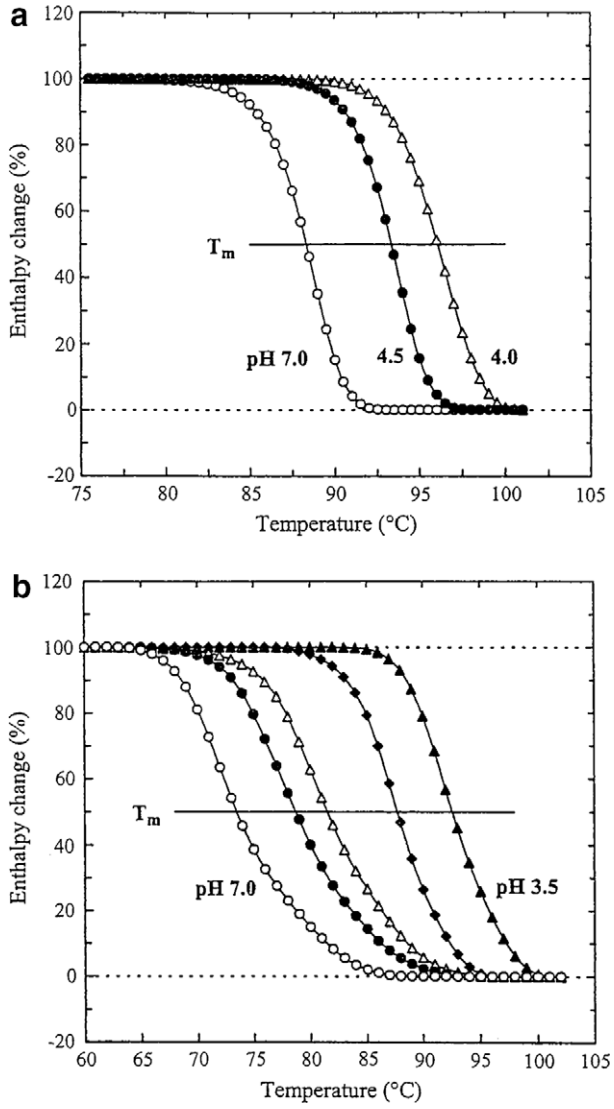

Fig. 8. Temperature-course of enthalpy change obtained by numerical integration of DSC peaks for 1.0 wt% solutions of (a) PFX (Fig. 7) and (b) commercial xanthan (Fig. 3) at pH values of 7.0 (○), 4.5 (●), 4.0 (△), 3.75 (◆) and 3.5 (▲). Transition-midpoint temperature (T_m) is taken as the temperature at which 50% of the change in enthalpy has occurred.

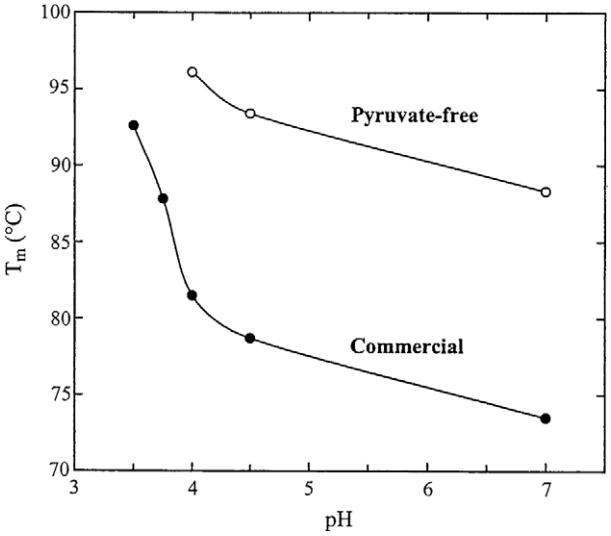

Fig. 9. Effect of pH on midpoint temperature (T_m) of the conformational transition of commercial xanthan (●) and PFX (○).

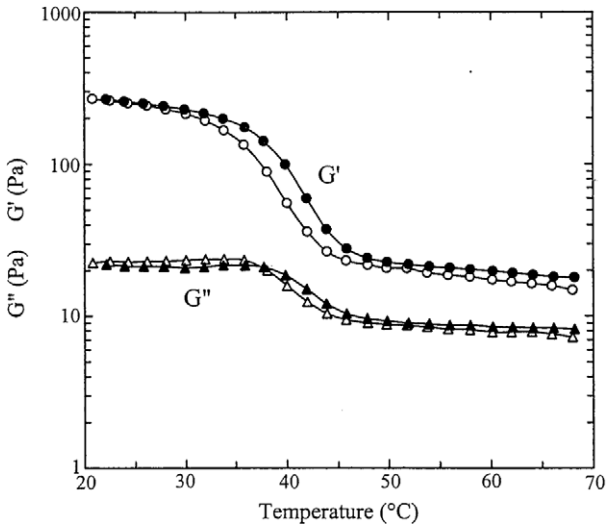

Fig. 10. Changes in G' (circles) and G'' (triangles), measured at 1 rad s^{-1} and 1% strain, for 0.5 wt% PFX in combination with 0.5 wt% KGM at pH 7.0, on cooling (open symbols) and heating (filled symbols) at 1.0 °C/min.

(by ~2 °C), which can again be explained by thermal lag. The averaged (absolute) values of heat flow from the heating and cooling scans, after subtraction of interpolated baselines (Fig. 13), are shown in Fig. 14. The temperature-course of thermal change at each pH was determined by the procedure of numerical integration described previously (Fig. 8) for commercial xanthan and PFX in the absence of KGM.

As illustrated in Fig. 15, the thermal transitions observed (Fig. 14) for mixtures of PFX and KGM follow roughly the same temperature-course as the changes in moduli (Fig. 11) which characterise formation and melting of the gel network. There is, however, only limited development of solid-like character (increase in G') above the midpoint temperature (T_m) from DSC, which is consistent with the requirement for significant intermolecular association to occur before a continuous network is formed (Clark & Ross-Murphy, 1987).

To allow the temperature-dependent rheological changes observed for PFX–KGM mixtures at different values of pH to be compared directly, the experimental curves from Fig. 11 were re-plotted with temperature (T) expressed relative to midpoint temperature from DSC (i.e. as $T - T_m$) and with experimental moduli divided by the values observed for the solution state at temperatures 30 °C above T_m. As shown in Fig. 16, the resulting plots of both G' (Fig. 16a) and G'' (Fig. 16b) superimpose well, indicating that reduction in pH, while lowering gelation temperature, does not fundamentally change the mechanism of network formation.

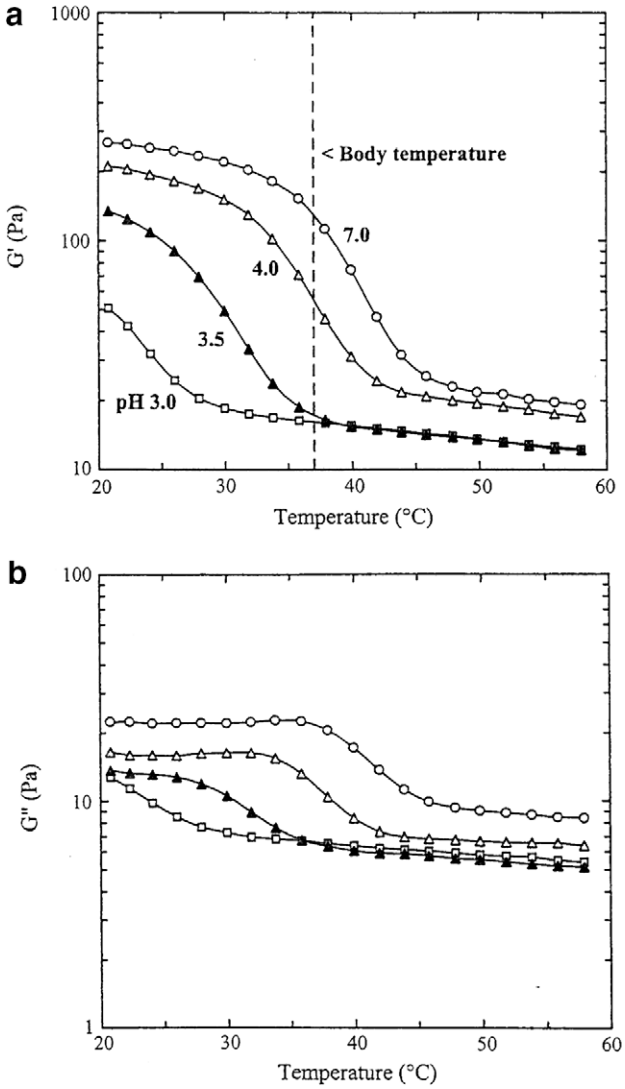

Fig. 11. Temperature-dependent changes in (a) G' and (b) G'' (1 rad s^{-1}; 1% strain; mean values from cooling and heating at 1.0 °C/min) for 0.5 wt% PFX in combination with 0.5 wt% KGM at pH values of 7.0 (○), 4.0 (△), 3.5 (▲) and 3.0 (□).

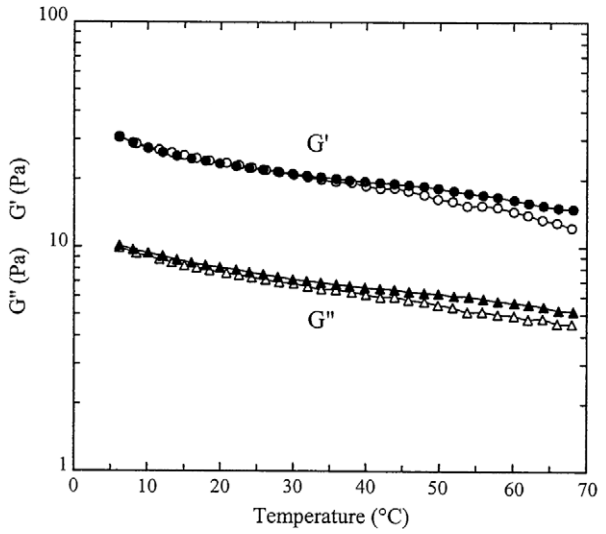

Fig. 12. Changes in G' (circles) and G'' (triangles), measured at 1 rad s^{-1} and 1% strain, for 0.5 wt% PFX in combination with 0.5 wt% KGM at pH 2.5, on cooling (open symbols) and heating (filled symbols) at 1.0 °C/min.

Finally, the studies of KGM with PFX provide a simple explanation for the two "waves" of increase in G' observed (Fig. 2) in gelation of mixtures of KGM with commercial xanthan at intermediate values of pH. Fig. 17 shows a direct comparison of the temperature-dependent changes in G' observed for mixtures of KGM with commercial xanthan and with PFX at pH 4.5. As described previously, increase in G' for the mixture of KGM with commercial xanthan occurs in two discrete steps. The first begins at ~60 °C, as observed (Fig. 1) at neutral pH; the second follows essentially the same temperature-course (Fig. 17) as the single increase in G' observed for the KGM–PFX mixture at the same pH. The obvious interpretation is that the first "wave" of gel formation comes from interaction of KGM with xanthan sequences that have retained a high content of pyruvate substituents and the second from interaction with sequences that have lost sufficient pyruvate (by acid hydrolysis) to behave in essentially the same way as the pyruvate-free material. On further reduction in pH, gelation of KGM with commercial xanthan occurs in one step, which, as illustrated in Fig. 18a and 18 b for mixtures prepared at pH 4.0 and 3.5, respectively, occurs over roughly the same temperature-range as gelation of KGM–PFX mixtures at the same values of pH, indicating extensive loss of pyruvate groups under these more strongly acidic conditions.

4. Discussion and conclusions

For both commercial xanthan (Fig. 3) and PFX (Fig. 6) the disorder–order transition moves to progressively higher temperatures with decreasing pH, until eventually it is displaced to above 100 °C. It seems likely that this is due to conversion of carboxylate groups from the ionised to the un-ionised form ($COO^- + H^+ \rightarrow COOH$), with consequent suppression of electrostatic repulsion between xanthan sidechains and, as discussed later, reduction in immobilisation of counterions. The increase in transition temperature, however, is accompanied by a progressive decrease in gelation temperature of mixtures with KGM (Figs. 2 and 11), and it seems reasonable to look for a causal relationship between these opposite trends.

As discussed in Section 1, two conflicting models have been proposed for interaction of KGM (or galactomannans) with xanthan: (i) attachment to the surface of the 5-fold helix, and (ii) binding to the cellulosic backbone of the xanthan molecule. These models came from research groups in, respectively, Unilever Research, Colworth Laboratory, Bedford, UK and the Institute of Food Research, Norwich, UK. In terms of the "Unilever" model, it could be argued that interaction of xanthan with KGM occurs in competition with self-association of xanthan helices,

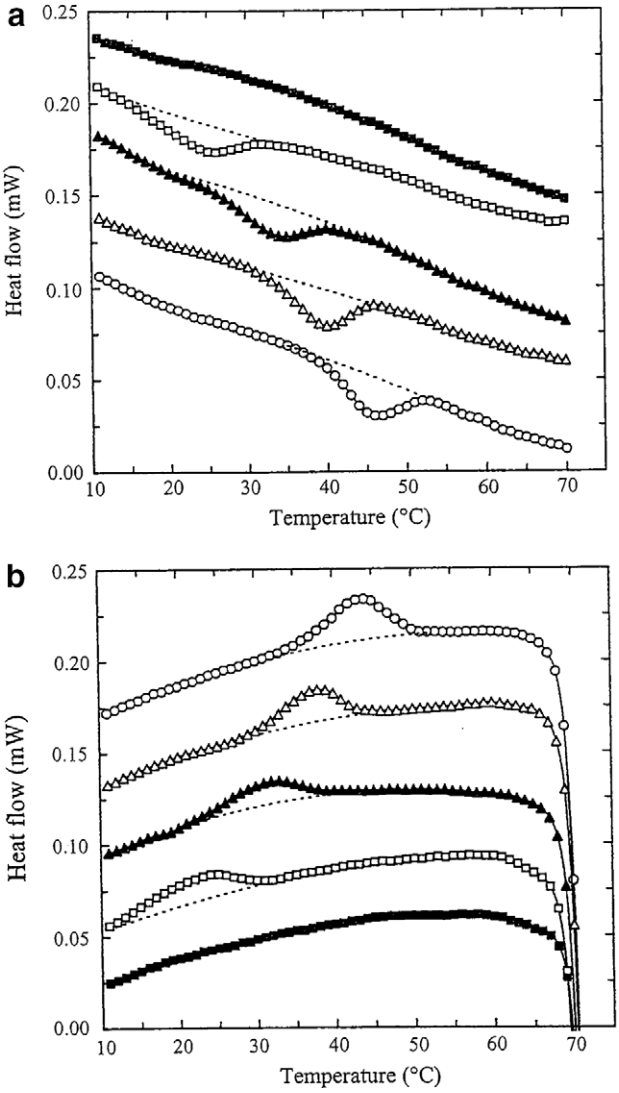

Fig. 13. DSC curves obtained for 0.5 wt% PFX in combination with 0.5 wt% KGM on (a) heating and (b) cooling (0.5 °C/min) at pH values of 7.0 (○), 4.0 (△), 3.5 (▲), 3.0 (□) and 2.5 (■). The dotted curves show interpolated baselines used in calculation of peak area. For clarity of presentation, the individual traces have been displaced vertically by arbitrary amounts.

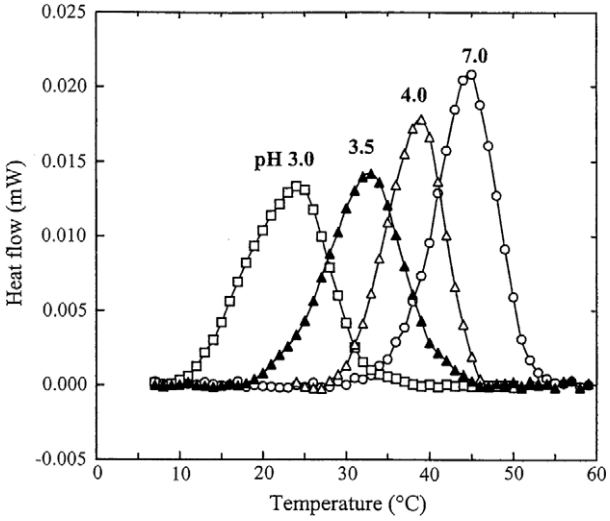

Fig. 14. Averaged (absolute) values of heat flow from the DSC heating and cooling scans in Fig. 13, after subtraction of interpolated baselines.

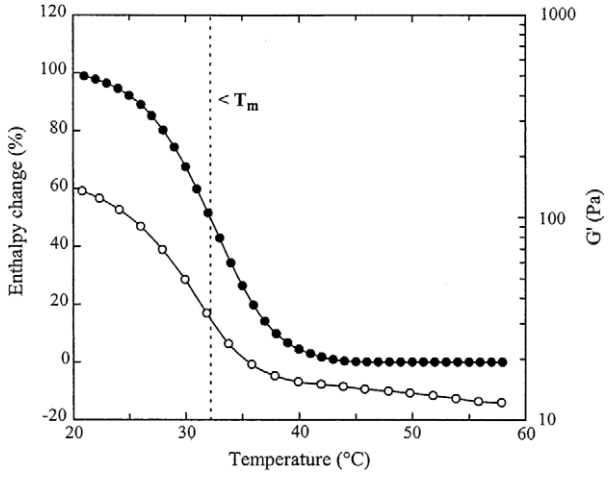

Fig. 15. Temperature-dependent change in G' (○; right-hand axis) in comparison with thermal change from DSC (●; left-hand axis), illustrated for 0.5 wt% PFX in combination with 0.5 wt% KGM at pH 3.5. Both curves are mean values from heating and cooling. The vertical dotted line shows midpoint temperature (T_m) from DSC.

and that self-association is promoted by reduction in electrostatic repulsion with decreasing pH. The "Norwich" model, however, seems to provide a more direct and convincing explanation of the inverse correlation between thermal stability of the xanthan helix and the temperature at which gels are formed on cooling in the presence of KGM. As the stability of the helix increases, its resistance to unfolding to allow KGM chains to bind to the cellulosic backbone would also be expected to increase, which is entirely consistent with the changes we have observed on varying pH.

It is also consistent with the results obtained for commercial xanthan and PFX at neutral pH. The disorder–order transition for PFX at pH 7.0 is substantially higher (Fig. 5) than for commercial xanthan (by ~16 °C) and, as can be seen from comparison of Figs. 1 and 11, the onset temperature for gelation with KGM is substantially lower (by ~14 °C). An inverse correlation between synergistic gelation and stability of the helix structure was also observed by Foster and Morris (1994) in an investigation of mixtures of LBG or KGM with commercial xanthan, deacetylated xanthan, and xanthan polytetramer, a genetically-engineered variant in which the terminal mannose residues of the sidechains are absent. Furthermore, Annable, Williams, and Nishinari (1994) found that addition of salts, which also increases the thermal stability of the xanthan helix, produced large (up to ~12 °C) reductions in the gelation temperature of xanthan–KGM mixtures.

To within the precision of our experimental results, the increase in order–disorder transition temperature with decreasing pH (Fig. 8), and the higher transition

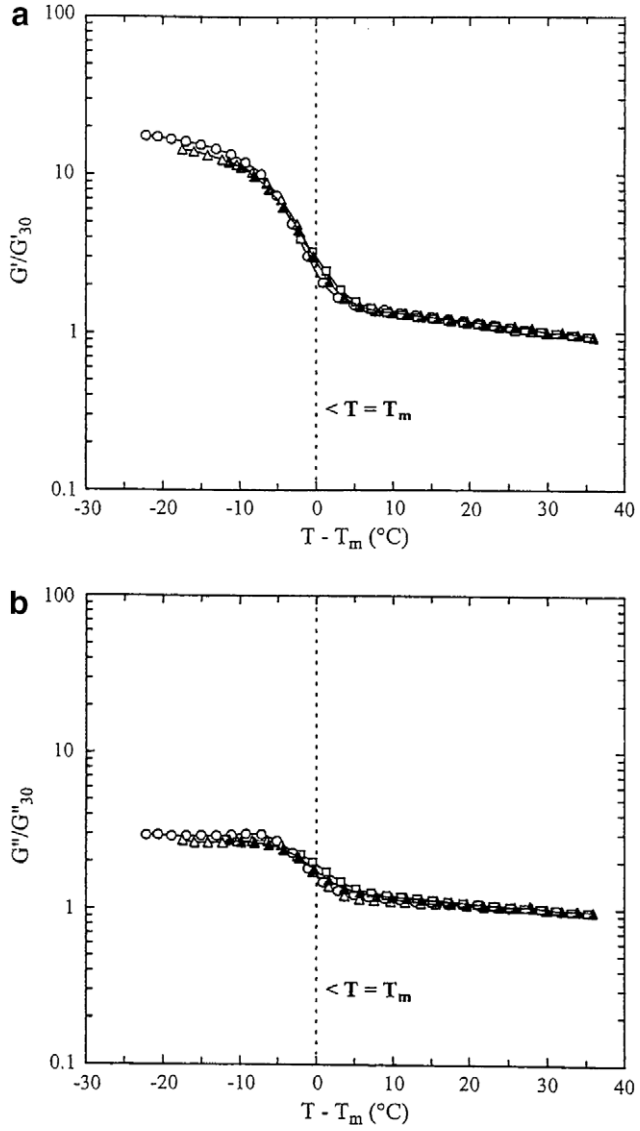

Fig. 16. Temperature-dependent changes in (a) G' and (b) G'' for 0.5 wt% PFX with 0.5 wt% KGM (Fig. 11) re-scaled by plotting temperature (T) relative to the midpoint temperature (T_m) from DSC (as $T - T_m$) and by dividing experimental moduli by the values 30 °C above T_m (G'_{30} and G''_{30}). Symbols as in Fig. 11.

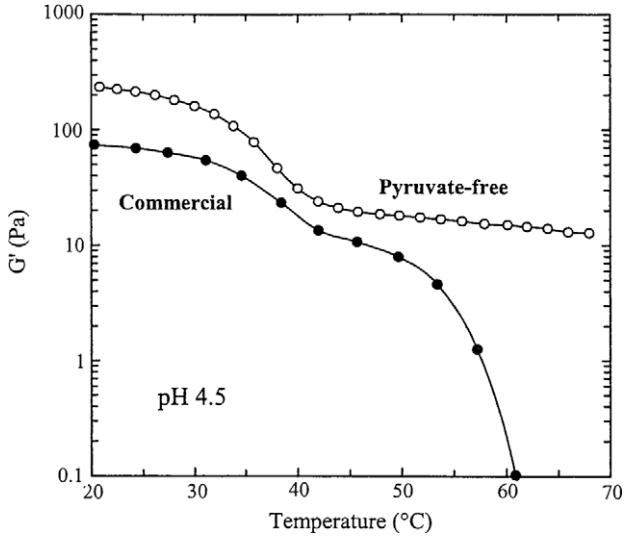

Fig. 17. Temperature-dependence of G' (1 rad s^{-1}; 1% strain) for 0.5 wt% PFX with 0.5 wt% KGM at pH 4.5 (○), in comparison with the curve obtained (Fig. 2) for the mixture of KGM with commercial xanthan at the same pH (●).

temperatures observed (Fig. 9) for PFX in comparison with commercial xanthan, cannot be related directly to an increase in enthalpic stability of the ordered conformation. As shown in Table 1, there is no discernable systematic variation in ΔH for the conformational transition of either commercial xanthan or PFX with varying pH, and the mean value for PFX is slightly lower than for commercial xanthan (6.9 ± 0.6 J/g, in comparison with 8.0 ± 1.0 J/g). Similarly, the reduction in sol–gel transition temperature with decreasing pH observed (Fig. 11) for mixtures of PFX with KGM is not reflected in any detectable systematic change in ΔH (Table 1) for the accompanying thermal transition (mean value 4.6 ± 0.5 J/g PFX). These apparent anomalies may, however, be explained by quantitative consideration of the factors affecting T_m.

As in any chemical process, transition-midpoint temperatures for formation and dissociation of polysaccharide ordered structures are determined by the following standard relationships:

$$\Delta G = \Delta H - T\Delta S = 0 \text{ at } T_m \quad (2)$$

$$\text{therefore : } T_m = \Delta H/\Delta S \quad (3)$$

where ΔH, ΔS and ΔG denote changes in, respectively, enthalpy, entropy and Gibbs free energy. Thus an increase in T_m can come from an increase in ΔH and/or a reduction in ΔS. The pH-dependent changes in transition temperatures (Figs. 3 and 6), although substantial, are comparatively small when expressed as a fraction of the absolute temperatures on the Kelvin scale (as in Eqs. 2 and 3) and it is possible, therefore, that genuine changes in ΔH may be obscured by experimental scatter. The likely involvement of entropic factors, however, must also be considered.

Since conformational ordering of xanthan involves immobilisation of sidechains, it seems reasonable to expect that the consequent loss of entropy will decrease as the length of the sidechains decreases. This would explain why PFX, where the sidechains are shortened by the absence of pyruvate ketal groups on the terminal mannose residues, gives higher values of T_m than commercial xanthan, despite showing smaller values of ΔH (Table 1). It is also consistent with the higher T_m values observed (Foster & Morris, 1994) for xanthan polytetramer in comparison with commercial xanthan. Adoption of the ordered structure might also be expected to cause loss of entropy by immobilisation of counterions to the carboxylate groups of the polymer. This effect should decrease as the charge on the polymer is decreased by reduction in pH, and may be a contributing factor to the observed increases in T_m.

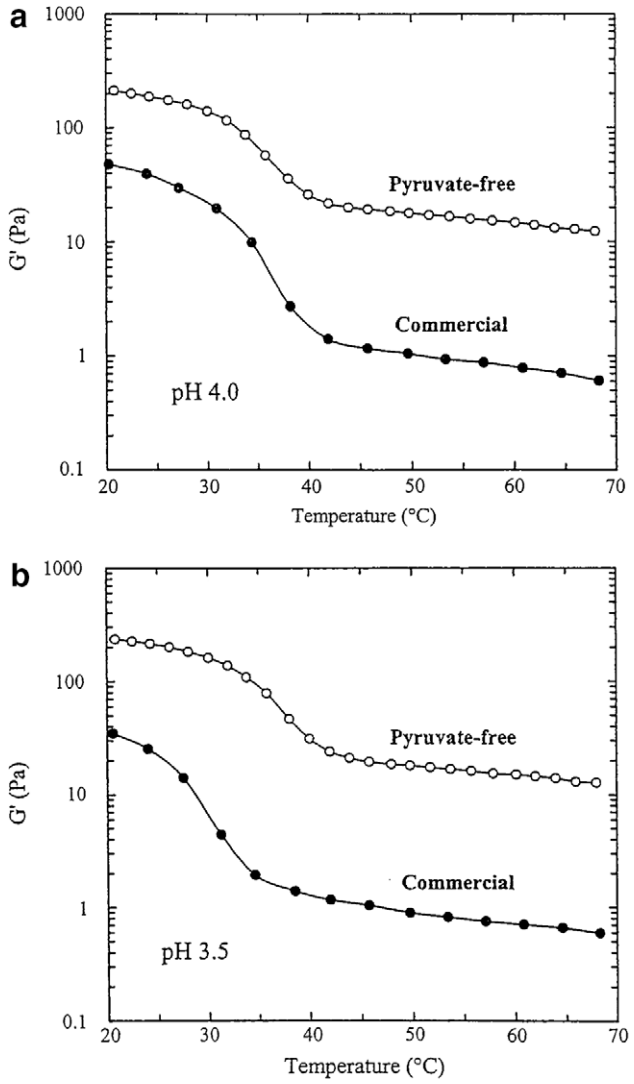

Fig. 18. Comparison of the temperature-dependence of G' for mixtures of KGM with PFX (○; Fig. 11a) or commercial xanthan (●; Fig. 2) at (a) pH 4.0 and (b) pH 3.5.

The ''Norwich'' model, which in the above interpretation is assumed to be correct, was based on two main lines of experimental evidence: (i) X-ray diffraction from oriented specimens of xanthan with galactomannans or with KGM gave intensities that did not appear in the diffraction patterns of either component in isolation, and (ii) solutions mixed at low temperature remained fluid, but gave a cohesive gels after heating to a temperature at which the xanthan component was converted to the disordered form, and then re-cooling. The second of these observations was interpreted as showing that interaction can occur only when the xanthan chains are disordered. However, this seems an unnecessary embellishment of an otherwise convincing model, and is inconsistent with the results of the present investigation.

As shown in Fig. 8a, conformational ordering of PFX at pH 7.0 is essentially complete by ~80 °C, but gelation with KGM (Fig. 11) does not begin until well below 50 °C. This already large separation between the temperature-range of conformational ordering and the onset of synergistic gelation increases progressively with decreasing pH, until at pH 3.5 the disorder–order transition is displaced to above 100 °C (Fig. 6), whereas gelation with KGM (Fig. 11) does not start until ~40 °C, which makes involvement of disordered sequences of the xanthan polysaccharide totally implausible. Synergistic gelation at temperatures well below the disorder–order transition of the xanthan component has been reported previously for mixtures with LBG (Mannion et al., 1992) and with KGM (Cronin, Giannouli, McCleary, Brooks, & Morris, 2002; Goycoolea et al., 1995), but the results presented here (Figs. 6 and 11) for mixtures of pyruvate-free xanthan with KGM at low pH provide a particularly clear demonstration that formation of a synergistic network does not require the xanthan component to be in its disordered form. As argued elsewhere (Morris, 1995; Morris & Foster, 1994), a much simpler explanation of why mixing xanthan with galactomannans or KGM at temperatures below the gelation temperature does not give cohesive gels is that the mixing process prevents formation of a continuous network (in much the same way as calcium alginate gels cannot be produced by simply stirring a solution of a calcium salt into a cold solution of sodium alginate).

In addition to their scientific interest, the results of this investigation may be of some practical significance. As shown in Fig. 11a, there is a large reduction in strength when mixed gels prepared in the pH range 4.0–3.5 are heated from a typical room temperature of ~20 °C to normal body temperature (~37 °C), but the initial moduli at 20 °C remain comparable to those obtained at neutral pH. The traces in Fig. 11 are for mixtures of KGM with pyruvate-free xanthan but, as shown in Fig. 18, closely similar temperature-dependence was observed at the same values of pH (4.0–3.5) for mixed gels formed by KGM with commercial xanthan on cooling from the loading temperature of ~85 °C (which, as discussed in Section 3, can be attributed to substantial loss of pyruvate groups even under these comparatively mild conditions of temperature and pH).

Gelatin is essentially unique among food-approved gelling agents in giving networks that soften or melt at body temperature, but its applications are limited by concerns about BSE and because it is unacceptable to vegetarians and to religious groups with prohibitions on consumption of products from cattle or pigs (notably Hindus, Muslims and Jews). Our present results suggest that mixtures of xanthan and KGM could provide a useful replacement, with none of the limitations on use, in applications where ''melt-in-the-mouth'' characteristics are important for product quality, and where moderate acidity is acceptable or necessary (e.g. fruit jellies).

Acknowledgements

This publication has emanated from research conducted with the financial support of Science Foundation Ireland.

The work presented in Figs. 1 and 2 formed part of the Ph.D. research of Dr. Alan M. Smith, which was generously sponsored by the Capsugel Division of Warner-Lambert. We thank Dr. Ross Clark of CP Kelco, San Diego, CA, USA for kindly providing the sample of pyruvate-free xanthan.

References

Annable, P., Williams, P. A., & Nishinari, K. (1994). Interaction in xanthan–glucomannan mixtures and the influence of electrolyte. *Macromolecules, 27*, 4204–4211.

Bradshaw, I. J., Nisbet, B. A., Kerr, M. H., & Sutherland, I. W. (1983). Modified xanthan – its preparation and viscosity. *Carbohydrate Polymers, 3*, 23–38.

Brownsey, G. J., Cairns, P., Miles, M. J., & Morris, V. J. (1988). Evidence for intermolecular binding between xanthan and the glucomannan konjac mannan. *Carbohydrate Research, 176*, 329–334.

Cairns, P., Miles, M. J., & Morris, V. J. (1986). Intermolecular binding of xanthan gum and carob gum. *Nature (London), 322*, 89–90.

Cairns, P., Miles, M. J., Morris, V. J., & Brownsey, G. J. (1987). X-ray fibre-diffraction studies of synergistic, binary polysaccharide gels. *Carbohydrate Research, 160*, 411–423.

Callet, F., Milas, M., & Rinaudo, M. (1987). Influence of acetyl and pyruvate contents on rheological properties of xanthan in dilute solution. *International Journal of Biological Macromolecules, 9*, 291–293.

Cheetham, N. W. H., McCleary, B. V., Teng, G., Lum, F., & Maryanto (1986). Gel-permeation studies on xanthan–galactomannan interactions. *Carbohydrate Polymers, 6*, 257–268.

Clark, A. H., & Ross-Murphy, S. B. (1987). Structural and mechanical properties of biopolymer gels. *Advances in Polymer Science, 83*, 57–192.

Cronin, C. E., Giannouli, P., McCleary, B. V., Brooks, M., & Morris, E.R. (2002). Formation of strong gels by enzymic debranching of guar gum in the presence of ordered xanthan. In P. A. Williams & G. O. Phillips (Eds.), *Gums and stabilisers for the food industry 11* (pp. 289–296). Cambridge, UK: Royal Society of Chemistry.

Davé, V., & McCarthy, S. P. (1997). Review of konjac glucomannan. *Journal of Environmental Polymer Degradation, 5*, 237–241.

Dea, I. C. M., & Morrison, A. (1975). Chemistry and interactions of seed galactomannans. *Advances in Carbohydrate Chemistry and Biochemistry, 31*, 241–312.

Dea, I. C. M., Morris, E. R., Rees, D. A., Welsh, E. J., Barnes, H. A., & Price, J. (1977). Associations of like and unlike polysaccharides: mechanism and specificity in galactomannans, interacting bacterial polysaccharides, and related systems. *Carbohydrate Research, 57*, 249–272.

Fitzsimons, S. M., Agoub, A. A., Giannouli, P., Mulvihill, D. M., & Morris, E. R. (2005). Gel formation from single-phase biopolymer mixtures. In *Gums and stabilisers for the food industry 13*, Wrexham, UK, July 2005.

Foster, T. J., & Morris, E. R. (1994). Xanthan polytetramer: conformational stability as a barrier to synergistic interaction. In G. O. Phillips, P. A. Williams, & D. J. Wedlock (Eds.). *Gums and stabilisers for the food industry 7* (pp. 281–289). Oxford, UK: IRL Press.

Goycoolea, F. M., Foster, T. J., Richardson, R. K., Morris, E. R., & Gidley, M. J. (1994). Synergistic gelation of galactomannans or konjac glucomannan: binding or exclusion?. In G. O. Phillips, P. A. Williams, & D. J. Wedlock (Eds.). *Gums and stabilisers for the food industry 7* (pp. 333–344). Oxford, UK: IRL Press.

Goycoolea, F. M., Richardson, R. K., Morris, E. R., & Gidley, M. J. (1995). and conformation of xanthan in synergistic gelation with locust bean gum or konjac glucomannan. *Macromolecules, 28*, 8308–8320.

Holzwarth, G. (1976). Conformation of the extracellular polysaccharide of *Xanthomonas campestris*. *Biochemistry, 15*, 4333–4339.

Jansson, P.-E., Kenne, L., & Lindberg, B. (1975). Structure of the extracellular polysaccharide from *Xanthomonas campestris*. *Carbohydrate Research, 45*, 275–282.

Mannion, R. O., Melia, C. D., Launay, B., Cuvelier, G., Hill, S. E., Harding, S. E., et al. (1992). Xanthan/locust bean gum interactions at room temperature. *Carbohydrate Polymers, 19*, 91–97.

Melton, L. D., Mindt, L., Rees, D. A., & Sanderson, G. R. (1976). Covalent structure of the extracellular polysaccharide from *Xanthomonas campestris*: evidence from partial hydrolysis studies. *Carbohydrate Research, 46*, 245–257.

Milas, M., & Rinaudo, M. (1979). Conformational investigation on the bacterial polysaccharide xanthan. *Carbohydrate Research, 76*, 189–196.

Milas, M., & Rinaudo, M. (1986). Properties of xanthan gum in aqueous solutions: role of the conformational transition. *Carbohydrate Research, 158*, 191–204.

Moorhouse, R., Walkinshaw, M. D., & Arnott, S. (1977). Xanthan gum – molecular conformation and interactions. *American Chemical Society Symposium Series, 45*, 90–102.

Morris, E. R. (1973). Polysaccharide conformation as a basis of food structure. In G. G. Birch & L. F. Green (Eds.), *Molecular structure and function of food carbohydrate* (pp. 125–132). London: Applied Science.

Morris, E. R. (1990). Mixed polymer gels. In P. Harris (Ed.), *Food gels* (pp. 291–359). London: Elsevier.

Morris, E. R. (1995). Polysaccharide synergism – more questions than answers?. In S. E. Harding S. E. Hill, & J. R. Mitchell (Eds.), *Biopolymer mixtures* (pp. 247–288). Nottingham, UK: Nottingham University Press.

Morris, E. R., & Foster, T. J. (1994). Role of conformation in synergistic interactions of xanthan. *Carbohydrate Polymers, 23*, 133–135.

Morris, E. R., Rees, D. A., Young, G., Walkinshaw, M. D., & Darke, A. (1977). Order–disorder transition for a bacterial polysaccharide in solution. A role for polysaccharide conformation in recognition between *Xanthomonas* pathogen and its plant host. *Journal of Molecular Biology, 110*, 1–16.

Morris, V. J. (1992). Designing polysaccharides for synergistic interactions. In G. O. Phillips, P. A. Williams, & D. J. Wedlock (Ed.). *Gums and stabilisers for the food industry 6* (pp. 161–171). Oxford, UK: IRL Press.

Nishinari, K., Williams, P. A., & Phillips, G. O. (1992). Review of the physico-chemical characteristics and properties of konjac mannan. *Food Hydrocolloids, 6*, 199–222.

Norton, I. T., Goodall, D. M., Frangou, S. A., Morris, E. R., & Rees, D. A. (1984). Mechanism and dynamics of conformational ordering in xanthan polysaccharide. *Journal of Molecular Biology, 175*, 371–394.

Okuyama, K., Arnott, S., Moorhouse, R., Walkinshaw, M. D., Atkins, E. D. T., & Wolf-Ullish, C. (1980). Fibre diffraction studies of bacterial polysaccharides. *American Chemical, Society Symposium Series, 141*, 411–427.

Piculell, L., & Nilsson, S. (1990). Effects of salts on association and conformational equilibria of macromolecules in solution. *Progress in Colloid and Polymer Science, 82*, 198–210.

Pramoda, M. K., & Lin, S.-L. (1979). Mixed xanthan gum and locust bean gum therapeutic compositions. US Patent 4,136,173.

Ross-Murphy, S. B. (1984). Rheological methods. In H. W.-S. Chan (Ed.), *Biophysical methods in food research. Critical reports on applied chemistry* (pp. 195–290). London, UK: SCI.

Ross-Murphy, S. B., Morris, V. J., & Morris, E. R. (1983). Molecular viscoelasticity of xanthan polysaccharide. *Faraday Symposia of the Chemical Society, 18*, 115–129.

Smith, A. M. (2002). Polysaccharide substitutes for gelatin in the production of pharmaceutical capsules. Ph.D. thesis, Cranfield University, Bedford, UK.

Smith, I. H., Symes, K. C., Lawson, C. J., & Morris, E. R. (1981). Influence of the pyruvate content of xanthan on macromolecular association in solution. *International Journal of Biological Macromolecules, 3*, 129–134.

Tolstoguzov, V. B. (1991). Functional properties of food proteins and role of protein–polysaccharide interaction. *Food Hydrocolloids, 4*, 429–468.